

RESEARCH ARTICLE | *Control of Coordinated Movements*

Intermuscular coherence reflects functional coordination

Christopher M. Laine and Francisco J. Valero-Cuevas

Brain-Body Dynamics Laboratory, Department of Biomedical Engineering, Division of Biokinesiology and Physical Therapy, University of Southern California, Los Angeles, California

Submitted 21 March 2017; accepted in final form 27 June 2017

Laine CM, Valero-Cuevas FJ. Intermuscular coherence reflects functional coordination. *J Neurophysiol* 118: 1775–1783, 2017. First published June 28, 2017; doi:10.1152/jn.00204.2017.—Coherence analysis has the ability to identify the presence of common descending drive shared by motor unit pools and reveals its spectral properties. However, the link between spectral properties of shared neural drive and functional interactions among muscles remains unclear. We assessed shared neural drive between muscles of the thumb and index finger while participants executed two mechanically distinct precision pinch tasks, each requiring distinct functional coordination among muscles. We found that shared neural drive was systematically reduced or enhanced at specific frequencies of interest (~10 and ~40 Hz). While amplitude correlations between surface EMG signals also exhibited changes across tasks, only their coherence has strong physiological underpinnings indicative of neural binding. Our results support the use of intermuscular coherence as a tool to detect when coactivated muscles are members of a functional group or synergy of neural origin. Furthermore, our results demonstrate the advantages of considering neural binding at 10, ~20, and >30 Hz, as indicators of task-dependent neural coordination strategies.

NEW & NOTEWORTHY It is often unclear whether correlated activity among muscles reflects their neural binding or simply reflects the constraints defining the task. Using the fact that high-frequency coherence between EMG signals (>6 Hz) is thought to reflect shared neural drive, we demonstrate that coherence analysis can reveal the neural origin of distinct muscle coordination patterns required by different tasks.

EMG; coherence, muscle synergies, coordination, correlation

APPROPRIATE COORDINATION of multiple muscles is essential for the nervous system to successfully perform mechanical tasks. Muscle coordination is often studied in terms of correlated patterns of EMG (Tresch and Jarc 2009; Giszter 2015). However, it is critical to develop signal processing techniques that can distinguish incidental descriptive correlations among EMG signals from prescriptive neural strategies (Bizzi and Cheung 2013; Brock and Valero-Cuevas 2016; Kutch and Valero-Cuevas 2012; Laine et al. 2015; Nazarpour et al. 2012; Tresch and Jarc 2009).

A means to approach this problem comes from the suggestion that muscles which are functionally “bound” by the nervous system in fact share a common neural drive (Farmer

1998). When different motor units share a common neural drive, their activities are simultaneously influenced by (and therefore synchronized by) that common drive (De Luca et al. 1982; Farina et al. 2016; Farmer et al. 1993; Sears and Stagg 1976). Intermuscular coherence has emerged as the statistical tool of choice to characterize such binding. In contrast to time-domain correlation methods, coherence can quantify the full frequency spectrum of synchronization between signals. This technique has been used to establish that muscles receive oscillatory neural drive at many frequencies, including high frequencies between 6 and 50 Hz (Conway et al. 1995; Boonstra 2013; Erimaki and Christakos 2008; Farmer 1998; Farmer et al. 1993). However, given the low-pass filtering properties of muscle, the neuromechanical consequences of such high frequency neural drive to force generation are not well understood (Zajac 1989). Rather, it is possible that these high-frequency signals reflect activity within neural circuits that control task-specific muscle coordination (Aumann and Prut 2015; de Vries et al. 2016; Farmer 1998; Nazarpour et al. 2012). This would imply a close relationship between the muscle coordination required to meet the neuromechanical requirements of the task and the neural drive that they share.

To better understand the factors that shape the spectrum of neural drive shared between coactivated muscles, we recorded EMG from three muscles of the thumb and index finger during production of 1) dynamic, isometric scaling of pinch force; and 2) dynamic rotation of a pinched dial. Each task requires different patterns of coordination among muscles to produce the necessary motions and forces. This paradigm is motivated by the fact that the mechanical requirements (and therefore the necessary neural control strategies) for motion, force, and their combination are distinct (Keenan et al. 2009; Mah and Mussa-Ivaldi 2003; Rácz et al. 2012; Venkadesan and Valero-Cuevas 2008). Thus our work focuses on the general effects that fundamental mechanical differences between tasks have on muscle activity and coordination, independently of the precise motions and forces associated with task performance. The target muscles were first dorsal interosseous (FDI; index finger), flexor digitorum superficialis (FDS; index finger), and abductor pollicis brevis (APB; thumb). We used coherence analysis to characterize and quantify the spectral content of shared neural drive between each pair of muscles. At the same time, we determined the pair-wise overall linear correlation between muscle activation profiles using a standard Pearson’s correlation of their EMG. Our overall hypothesis was that spectral properties of coherence, as a measure of shared neural

Address for reprint requests and other correspondence: F. J. Valero-Cuevas, Brain-Body Dynamics Laboratory, Dept. of Biomedical Engineering, Div. of Biokinesiology and Physical Therapy, Univ. of Southern California, Los Angeles, 3710 South McClintock Ave., Los Angeles, CA 90089 (e-mail: valero@usc.edu).

drive, would reflect the changes in functional coordination of muscles across tasks.

METHODS

Experiments were carried out at the University of Southern California. All procedures were approved by the Institutional Review Board at the University of Southern California, and all participants gave written consent before participation. A total of 10 healthy adults (6 male, ages 24–36 yr) executed precision-pinch tasks with their self-reported dominant hand (9 right handed).

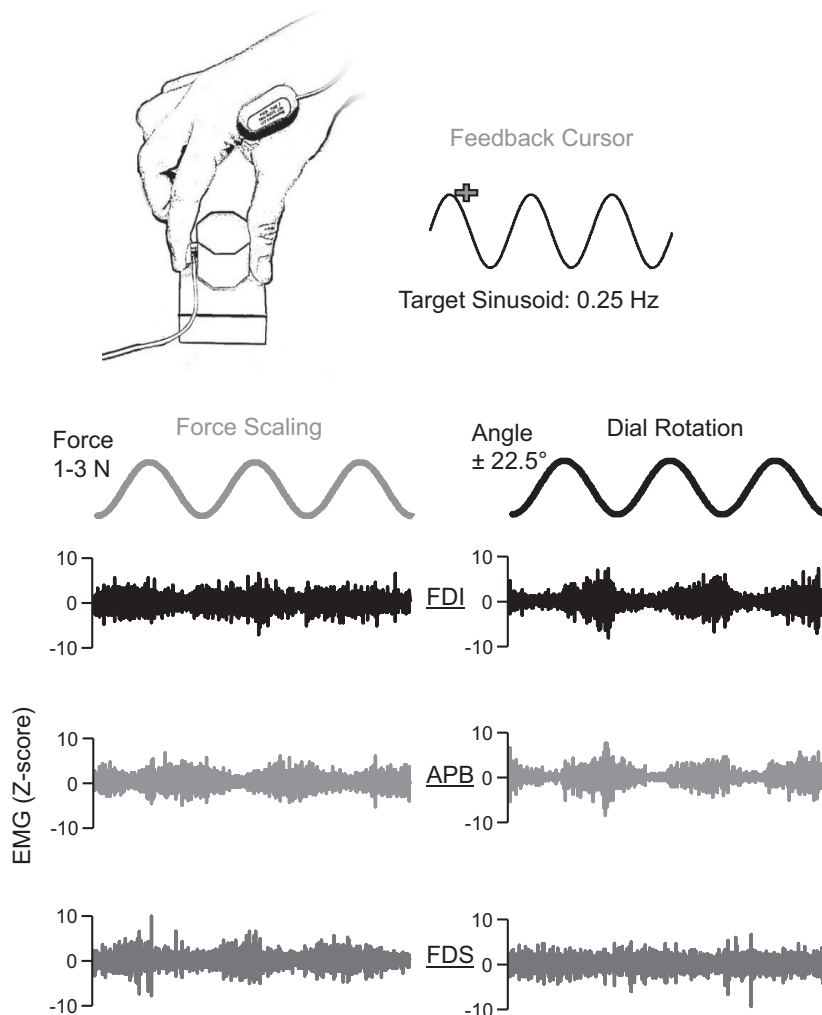
General setup. Participants were to pinch or rotate a custom-made octagonal dial (diameter: 3 cm), which was gripped between the thumb and index finger, as in Fig. 1, *top*. The elbow was rested on a comfortable pad to isolate hand function. All tasks were executed without movement of the wrist, arm pronation-supination was held constant, and participants were monitored to ensure that only the fingers were used to perform the tasks. A potentiometer within the dial was used to track rotation angle, and pinch forces were measured using a miniature load cell (ELB4–10, Measurement Specialties, Hampton, VA) placed on the dial at the position of the index finger. All signals were acquired, amplified, and recorded at 1,000 Hz using a biometrics LTD Datalink system and associated software (Biometrics, Newport, UK). A copy of the force and rotation signals was delivered to a national instruments data acquisition unit (National Instruments, Austin, TX) for use with custom visual feedback software designed in MATLAB (The MathWorks, Natick, MA). Biomet-

rics active bipolar surface EMG sensors were placed on 1) the first dorsal interosseous (FDI) muscle, between the thumb and index finger; 2) the abductor pollicis brevis (APB) on the thenar eminence of the palm; and 3) the flexor digitorum superficialis (FDS), roughly 7 cm proximal to the crease of the wrist, on the ulnar side. All sensors were placed on the dominant hand after the skin surface was cleaned with alcohol. A grounding strap was placed on the opposite wrist. Proper electrode positioning was established by physical palpation during isolated index finger abduction, thumb abduction, and index finger flexion, and confirmed by observation of the EMG signals during these activities.

Participants were given time to practice and familiarize themselves with each experimental task (described below). The tasks were not difficult, and one or two practice trials of ~30 s were typically sufficient to achieve accurate and stable performance. Direct quantification of task performance was not an aim of this study; however, we noted no obvious changes in task performance, or EMG activity across the duration of each trial, for either task. While variability in task performance across participants may contribute to interindividual variability in a variety of measures, full characterization of such effects was beyond the scope and design of this study.

Task 1: dynamic modulation of isometric force. In isometric pinching task, participants pinched a dial between the thumb and index finger and exert a slowly varying 1- to 3-N sinusoidal force. Visual feedback of exerted force was provided in the form a cursor that traveled left to right across the screen for 20 s before looping back to the left. The vertical height of the cursor represented the pinch force

Fig. 1. Experimental setup. A total of 10 participants were asked to complete 2 visually guided manipulation tasks. In the 1st task, participants produced an isometric pinch force that was scaled between 1 and 3 N following a 0.25-Hz sinusoidal target (4 s per cycle). Participants used visual feedback of their exerted pinch force to track the target displayed on a computer screen. Simultaneously, surface EMG signals were recorded from the first dorsal interosseous (FDI), abductor pollicis brevis (APB), and flexor digitorum superficialis (FDS). In the 2nd task, participants rotated a dial clockwise and counterclockwise over a small arc ($\pm 22.5^\circ$) while maintaining a pinch force between 1 and 3 N. The color of the feedback cursor would change if force exceeded this range; thus we guaranteed that subjects did not produce forces that were too high or too low. This warning allowed pinch force to be held at comparable levels across conditions. Each individual completed two 120-s trials of each target tracking task in random order. *Bottom:* the progression of EMG activity is shown for each muscle with respect to the phase of the target sinusoid over a 12-s epoch for a representative participant. *Left:* normalized EMG traces (see METHODS) for the force scaling task. *Right:* EMG traces recorded during dial rotation. The modulation of EMG activity showed changes across muscles and tasks.



exerted by the participants, and a sinusoid (0.25 Hz) was displayed to provide a target to track. Each participant completed two, 120-s trials of force tracking. This task required the control of the magnitude of isometric fingertip forces and was expected to produce strongly correlated activation of all muscles (Valero-Cuevas 2000).

Task 2: dial rotation. In the dial rotation task, subjects were required to rotate the dial back and forth between the thumb and index finger. This task required the simultaneous control of fingertip movements and forces (Rácz et al. 2012). The rotation of the dial, from the most counterclockwise position to the most clockwise position, spanned an angle of 45°. Visual feedback of rotation was displayed as a sinusoid on the computer screen, as described above. The cursor's vertical position was increased by increasing the degree of clockwise rotation. In order for pinch force to remain comparable with the other tasks, the cursor color was changed to gray if the total pinch force fell outside of the 1- to 3-N range. All participants were able to maintain their pinch forces within this range while tracing the sinusoidal target. This task was expected to produce synchronized activation of the FDI and APB muscles, which were both anticipated to show reduced coupling with the FDS, since the FDS does not produce the index finger ad/abduction required during dial rotation.

Data analysis. EMG signals were initially band-pass filtered between 20 and 460 Hz by the active EMG sensors, and then further filtered offline using a zero-phase 4th order high-pass Butterworth filter set at 250 Hz, following published recommendations (Boonstra and Breakspear 2012). High-pass filtering reduces action potentials to thin spikes, which reduces overlap between the frequency content of their 'shapes' and the frequency content of neural drive to the motor units (Boonstra and Breakspear 2012). Additionally, the procedure helps to reduce artifacts related to movement, filtering effects of skin and soft tissue, and volume conduction from nearby muscles (Brown et al. 2009; Potvin and Brown 2004; Riley et al. 2008; Staudenmann et al. 2007). The filtered signals were then full-wave rectified, as is often recommended for preparing EMG signals for correlation and coherence analysis (Boonstra and Breakspear 2012; Farina et al. 2013; Ward et al. 2013) and normalized to unit variance (z -score). Rectification emphasizes the grouping and timing of motor unit action potentials (short duration, high-frequency events) embedded within the surface EMG signals. Accordingly, intermuscular coherence analysis can provide a practical, informative, and noninvasive measure of motor unit synchronization between muscles, without having to fully decompose each EMG signal into trains of individual motor unit action potentials. For each participant, the EMG signals were concatenated across trials before further analysis.

EMG amplitude correlations. To assess the overall temporal correlation between any two muscles within each task, the rectified EMG signals for each muscle of each subject were low-pass filtered at 1 Hz (2nd-order Butterworth filter) and then used to calculate Pearson's correlation. This allowed us to extract the EMG envelope for each muscle and use correlation analysis to determine intermuscular task-level coordination as a benchmark for the subsequent coherence analysis. Since correlations can be either positive or negative, correlation strength was assessed using the absolute values of the correlation coefficients. The absolute-valued correlation coefficients were normalized using Fisher's r -to- z transform [$Fz = \text{atanh}(r)$] before statistical comparison.

Intermuscular coherence. Coherence is the frequency-domain extension of Pearson's correlation coefficient and expresses the degree of linear correlation between signals at each frequency on a scale of 0 to 1, with 0 representing no correlation and 1 representing perfect correlation. Coherence was initially calculated using the "mscohere" function in MATLAB, specifying segment sizes of 1 s (1,024 samples), without overlap, and rectangular windowing. As is customary, raw coherence values (C) were first transformed into standard z -scores using the formula: $z = \{ \text{atanh}(\sqrt{C})\sqrt{(1/2L)} \} - \text{bias}$, where L is the number of segments used in the coherence analysis and the bias is calculated empirically as the mean z -value between 100 and 500 Hz

(Baker et al. 2003; Laine et al. 2014; Rosenberg et al. 1989). This empirical method for bias removal assumes that the signals are uncorrelated within the specified range. For other signals, where such assumptions are uncertain, theoretical approaches (e.g., Bokil et al., 2007) could be employed. As with any z -test, the transformed coherence values can be considered significantly greater than zero at a value of 1.65 (one-sided 95% confidence level). It is worth noting that time-varying muscle contractions produce time-varying EMG amplitudes, which some authors attempt to remove (Boonstra et al. 2009; DeMarchis et al. 2015) before coherence analysis while others do not (Kakuda et al. 1999; Omlor et al. 2007; Semmler et al. 2002). While we cannot completely rule out any influence of muscle coordination on the statistical detection of shared neural drive (rather than its strength), we found that removing temporal variation in EMG amplitudes was unnecessary, given our particular task, choice of muscles, and EMG preprocessing methods. In fact, our standard coherence analysis produced qualitatively identical results to a pure phase-locking analysis (Lachaux et al. 1999), in which signal amplitudes are completely ignored. We therefore chose to present results from the more standard coherence analysis, as it is more easily comparable to similar literature and allows for a more straight-forward statistical evaluation.

We then averaged the z -transformed coherence profiles across all participants to assess the overall spectrum of shared drive between each muscle pair for each task. Averages over 0.52 exceed the 95% confidence level for the population. This is the value at which an average of 10 z -scores corresponds with a composite z -score of 1.65 (derived using Stouffer's z -score method, as in Kilner et al. 1999). In addition, histograms were constructed to show the number of participants with statistically significant coherence at each frequency. It is unlikely that any frequency component should show significant coherence in 3 or more of the 10 participants, since this would exceed the 5% chance level for 10 independent measurements, according to a binomial test.

To better evaluate the magnitude and variability of coherence across participants, we constructed box and whisker plots depicting the mean coherence obtained within each of three frequency bands of interest; 6 to 15, 16 to 29, and 30 to 50. The 6- to 15-Hz band is typically thought to reflect spinal reflex circuitry (Christakos et al. 2006; Erimaki and Christakos 2008; Lippold 1970), while the "beta" (16–29)- and "gamma" (30–50)-Hz bands are known to reflect cortical drive to muscles (Boonstra 2013; Farmer 1998; Mima and Hallett 1999).

EMG power. For completeness, we also quantified task-related changes in the EMG amplitudes power spectra across tasks. For each muscle, the raw EMG signal was filtered and rectified, as for the correlation and coherence analyses. To assess task-related changes in overall muscle activation, we calculated the mean rectified EMG amplitude for each muscle, in each condition, and recorded the rotation-to-scaling ratio for each participant. Then, a spectral analysis was carried out to reveal the proportions of total (rectified EMG) variance. Normalization to total signal power enables better comparison across individuals, whom may have different skin impedances, muscle sizes, etc.

Statistical comparisons. All task-related changes in EMG power, amplitude correlations, and coherence values were evaluated using a signed-rank test. This is a paired, conservative, nonparametric test of difference. For all tests, significance was initially set to the 95% confidence level. We used a Bonferroni-correction when evaluating the overall influence of task on the coherence spectrum, since three different frequency bands were tested. For each significant test result, we also report the rank statistic W and the rank correlation, r , as a measure of effect size. For W and r , positive values indicate that a given measure was larger in the scaling task compared with the rotation task. The rank correlation will have a maximal absolute value of 1 if all paired differences have the same sign.

RESULTS

General features of EMG during performance of each task. The activities of each muscle followed a temporal progression that varied according to task. Figure 1 shows, for each task, a 12-s epoch of normalized EMG signals recorded from one participant. To emphasize task-related EMG modulation and set signals onto an equal scale, the EMG traces for each participant were normalized to unit variance. Figure 1 is intended as illustrative; statistical evaluation of temporal correlations are described in detail below, along with pair-wise intermuscular coherence. Note that the temporal modulation of EMG depends on both muscle and task.

FDI (index finger abductor/flexor) to APB (thumb abductor) synchronization. The correlation of activation profiles between FDI and APB muscles was evaluated in Fig. 2, *top left*. The box plots show the median and interquartile ranges of the Pearson's correlation between both muscles across the 10 participants. The correlation switches sign between tasks (negative for force scaling and positive for dial rotation) but was not significantly different in absolute magnitude between the two tasks ($P = 0.19$).

In contrast, the strength of intermuscular coherence was highly dependent upon task. Figure 2, *top right*, shows the average z-transformed coherence across all participants. The rotation task clearly evoked stronger coherence, especially at ~10 and ~40 Hz. To be conservative, we not only report the group average but have also constructed a histogram depicting the number of participants who showed significant coherence at each frequency (Fig. 2, beneath the average coherence profile). The increased average coherence observed during dial rotation relative to force scaling is also reflected in the higher consistency of significant coherence. In Fig. 2, *bottom*, box-plots show the mean of coherence values found for each participant within each of three distinct frequency bands of interest. The 6- to 15-Hz and 30- to 50-Hz bands showed significantly larger mean coherence during dial rotation as compared with force scaling (6–15: $P = 0.0039$, $W = -53$, $r = -0.96$; 30–50: $P = 0.014$, $W = -47$, $r = -0.85$). The 16- to 29-Hz band showed a similar but much weaker trend ($P = 0.065$, $W = -37$, $r = -0.67$). Under the global null hypothesis that coherence is not influenced by task, none of the three statistical tests should show a $P < 0.017$ ($0.05/3$, as per

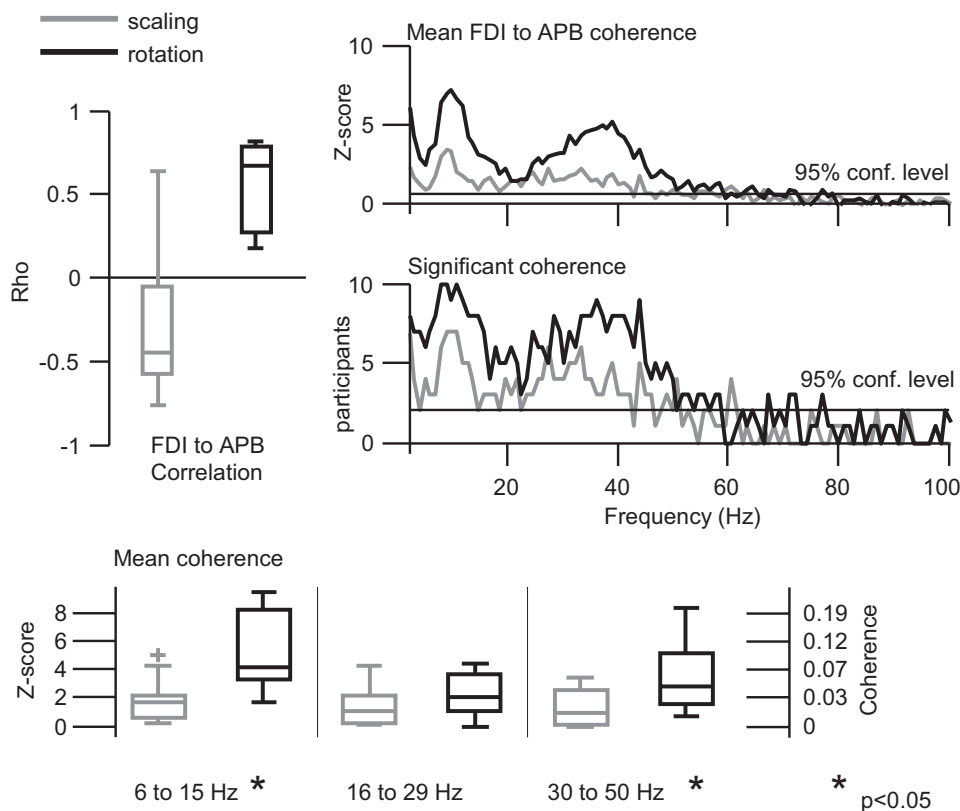


Fig. 2. FDI:APB synchronization. *Top left*: pair of boxplots depicts the Pearson's correlation between the EMG activities of the FDI and APB muscles over time within each task (gray, force scaling; black, dial rotation). Each box shows the median and interquartile ranges spanning the values obtained from the entire data set (1 value per participant). The FDI (acting on the index finger) and APB (acting on the thumb) muscles showed out-of-phase activity during force scaling, and thus their correlation coefficients are negative. The opposite relationship was found during dial rotation. The absolute magnitude of correlation was not significantly different between the tasks. *Right*: boxplots are the results of coherence analysis between the muscles. *Top traces*: mean coherence (z-score) at each frequency from 2 to 100 Hz. At nearly all frequencies up to 50 Hz, the average coherence was larger for the rotation task compared with the force scaling task. The horizontal line marks the 95% confidence level for the population average. Below the mean coherence plot is a histogram depicting the number of participants who had statistically significant coherence at each frequency. The horizontal line at 3 indicates that significant ($P < 0.05$) coherence occurred more frequently than would be expected by chance, given the 5% chance level associated with each test. *Bottom*: boxplots provide a description of the median/range of data obtained from each of the 10 participants. For this analysis, the mean coherence z-score was calculated for each individual within each of the 3 frequency ranges depicted. For reference, an axis at the *right* shows the raw coherence values that correspond to the calculated z-scores. There was a significant (Bonferroni-corrected $P < 0.05$) increase in 6- to 15-Hz and 30- to 50-Hz coherence during dial rotation as compared with force scaling. Statistical comparisons were conducted using a signed-rank test.

a Bonferroni correction). Both the 6- to 15-Hz and 30- to 50-Hz bands passed this significance level.

FDS (index finger flexor) to FDI (index finger abductor/flexor) synchronization. The same analyses as described above were carried out for the correlation and coherence between the FDS and FDI muscles, which are mechanically synergistic for the production of flexion torque at the metacarpophalangeal joint in this posture of the index finger (Valero-Cuevas et al. 1998). It can be seen from Fig. 3, *left*, that the FDS and FDI muscles are positively correlated during force scaling, and negatively correlated during dial rotation, which is opposite to the correlations between the FDI and APB muscles across tasks. In this case, the correlation magnitude is significantly stronger ($P = 0.0059$, $W = 51$, $r = 0.93$) during force scaling as compared with dial rotation.

The coherence profiles between FDS and FDI muscles (Fig. 3, *right*) show almost the reverse of Fig. 2, this time showing generally stronger and more consistent coherence for the force scaling task as compared with rotation. In terms of mean coherence within individual frequency bands (Fig. 3, *bottom*), these differences were highly significant at 6–15 Hz ($P = 0.0059$, $W = 51$, $r = 0.93$) and 30–50 Hz ($P = 0.0098$, $W = 49$, $r = 0.89$) and weaker at 16–29 Hz ($P = 0.049$, $W = 39$, $r = 0.71$). Again, both the 6- to 15-Hz and 30- to 50-Hz bands exceeded the Bonferroni-corrected significance level. Large peaks in coherence at ~40 Hz, which were common features of FDI to APB coherence during dial rotation, were never present between the FDS and FDI.

FDS (index finger abductor/flexor) to APB (thumb abductor) synchronization. Finally, the coupling between the FDS and APB muscles were also evaluated for each task. In both tasks, the correlations (Fig. 4, *left*) were relatively weak, both nega-

tive in sign, and were not significantly different in magnitude across the two tasks ($P = 0.49$).

In Fig. 4, *right*, it can be seen that coherence at all frequencies were very similar between the tasks as well, and in terms of consistency, very few participants showed significant coherence above 10 Hz, although it was more common than would be expected purely by chance. The boxplots in Fig. 4, *bottom*, confirm that there was little task-related modulation of FDS to APB coherence in any of the three frequency bands, with P values of 1.0, 0.49, and 0.11 for the 6- to 15-Hz, 16- to 29-Hz, and 30- to 50-Hz bands, respectively.

EMG amplitude and power spectra. The boxplots in Fig. 5, *left*, show the rotation-to-scaling ratio of overall EMG amplitudes for each muscle, across the 10 participants. For the most part, rotation elicited an increase in muscle activity for all muscles (ratios >1). The FDI muscle was more variable in this regard compared with the other muscles, since adduction of the index finger during dial rotation sometimes reduced FDI EMG activity more than index finger abduction increased it (relative to the force scaling task). To assess changes in EMG frequency content, we used the filtered, rectified, and normalized EMG signals recorded from each muscle to construct normalized power spectra. The distribution of power across frequencies was not strongly altered by task. The spectra in Fig. 5 show the mean (\pm SD) for each task. The vertical lines indicate frequencies which showed a significant difference ($P < 0.05$) across tasks, according to a signed-rank test. In general, there were no broad, significant increases or decreases in spectral power near ~10 or ~40 Hz, despite the consistent task-related modulation of these frequencies within the coherence profiles.

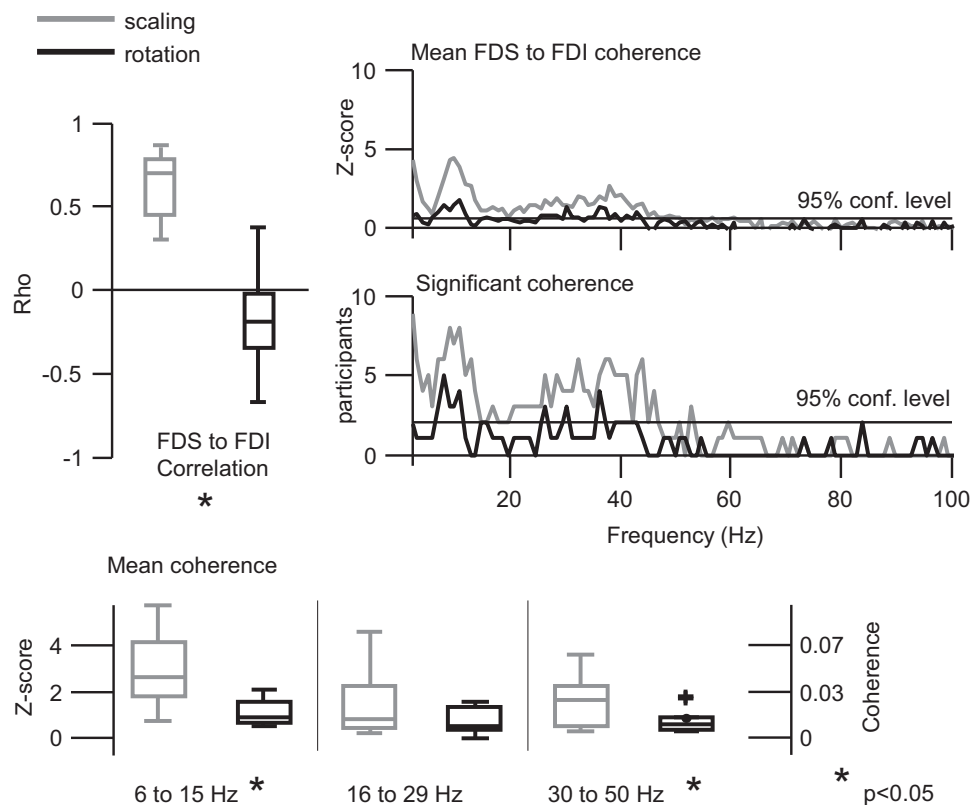
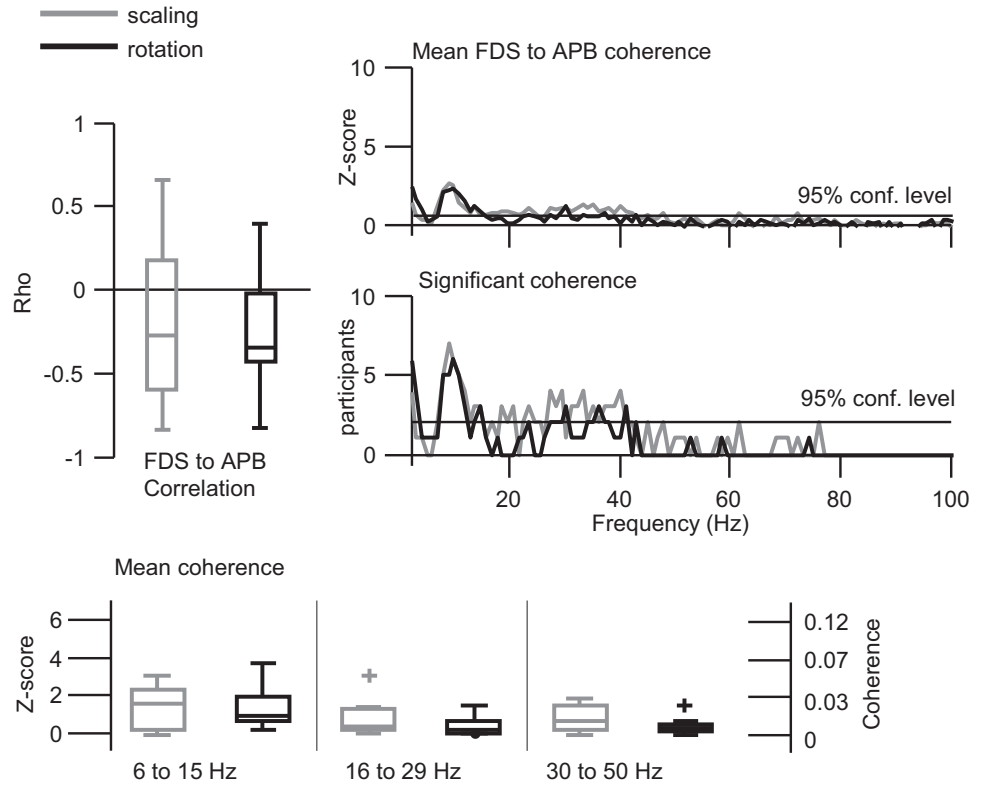


Fig. 3. FDS:FDI synchronization. The synchronization between the FDS and FDI muscles were analyzed as in Fig. 2. *Top left*: set of boxplots show the Pearson's correlation between the 2 muscles for each task. It can be seen that force scaling produced in-phase activation (positive correlation) of the 2 muscles whereas dial rotation was associated with out-of-phase activity (negative correlation). In this case, the absolute magnitude of the correlation was larger for the force scaling task as compared with the rotation task. *Right*: boxplots are the average coherence profiles (*top traces*) as well as coherence histograms (*bottom*). The average coherence and consistency of significant coherence were greater for force scaling at every frequency up to ~50 Hz. The pattern is essentially opposite what was observed between the FDI and APB muscles (Fig. 2). *Bottom*: boxplots show the spread of mean coherence values across participants for each frequency range. There was a significant (Bonferroni-corrected $P < 0.05$) decrease in 6- to 15-Hz and 30- to 50-Hz coherence during dial rotation as compared with force scaling. Statistical comparisons were conducted using a signed-rank test.

Fig. 4. FDS:APB synchronization. The synchronization between the FDS and APB muscles was analyzed as in Figs. 2 and 3. *Top left*: boxplots show the Pearson's correlation between the 2 muscles for each task. The 2 muscles were weakly and negatively correlated for both tasks, and the correlation magnitudes did not differ significantly according to task. Similarly, coherence was nearly identical between the 2 conditions at every frequency, both in terms of average coherence (*top right, top traces*) as well as the consistency of significant coherence across participants (*top right, bottom traces*). Furthermore, the mean coherence within each frequency range, shown in the boxplots at *bottom*, showed no difference across conditions. As in Figs. 2 and 3, statistical comparisons were conducted using a signed-rank test.

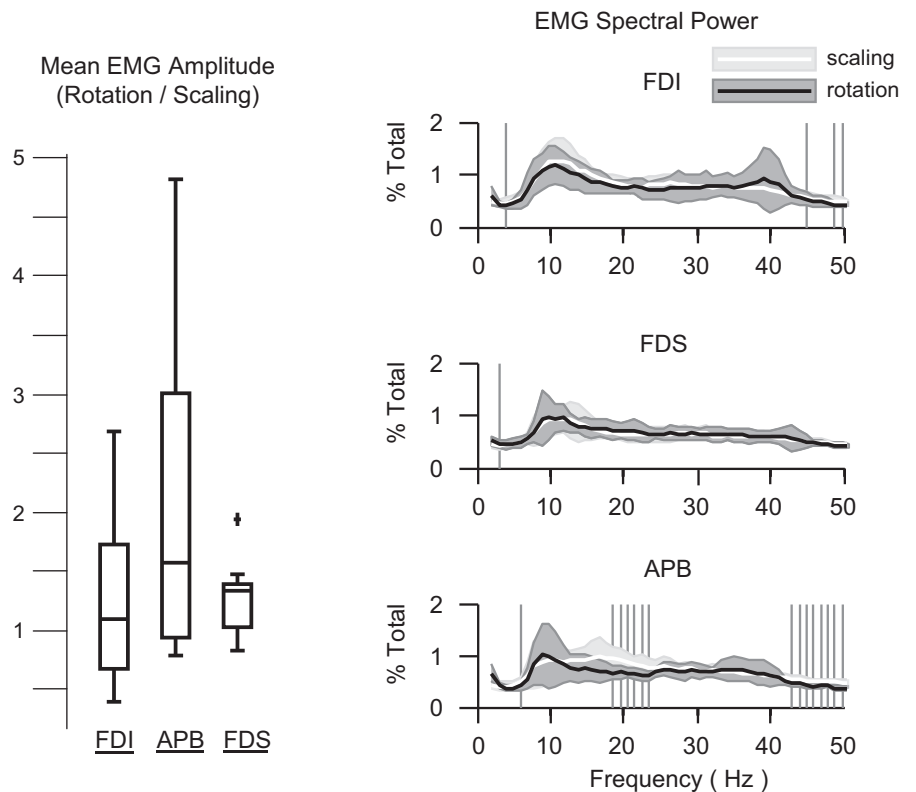


DISCUSSION

In this investigation, we characterized the strength, spectral properties, and coherence of EMG signals recorded from the FDI, FDS, and APB muscles during execution of two mechanically distinct manual tasks. Our results demonstrated that the

pattern of coordination between muscles at the slow time scale of each task was predictive of their “binding” by shared neural drive (intermuscular coherence) at much higher frequencies. The same was not true of the overall level muscle activation, the spectral power of the EMG signals, the presence or absence

Fig. 5. Amplitude and spectral power of FDI, FDS, and APB. *Left*: depicts how the mean rectified EMG signals for each muscle changed across tasks. The plots show the ratio of EMG amplitude during dial rotation relative to the force scaling condition. Rotation typically increased the overall activation of all muscles. *Right*: normalized power spectra depicting changes in the frequency content of the EMG signals across tasks. Means (solid lines) \pm 1 SD (shaded regions) for the normalized EMG power recorded from each muscle are shown. The traces represent the average percentage of total signal power at each frequency for dial rotation (black with dark shading) and force scaling (white with light shading). The dark vertical bars indicate 1-Hz frequency bins in which a significant ($P < 0.05$) difference in normalized power was observed across tasks. Interestingly, no significant shifts in spectral power occurred at the ~10- and ~40-Hz frequency ranges, where the majority of task-related modulation of coherence occurred. Shown is that neither changes in the frequency content of the EMG signals nor the overall amplitude of the EMG signals can explain changes in coherence between muscles, as assessed in Figs. 2–4.



of digit movement, or even the anatomical relationship between the muscles.

To interpret the results of this study, it is necessary to first describe the relationships, if any, which must exist between muscle coordination and shared neural drive. To start with, two independently-controlled muscles can show strong EMG amplitude correlations at the time-scale of a task, without any need for a shared input signal. Furthermore, shared input at relatively high frequencies (e.g., 10–50 Hz) would theoretically have little influence on the force produced by the muscles receiving such drive (Zajac 1989). In contrast, high-frequency shared input is interpreted as reflective of neural binding (Boonstra et al. 2015; Farmer 1998; McAuley and Marsden 2000). However, neither coherence (as a statistical measure) nor “neural binding” (as a neurophysiological concept) at these high frequencies necessarily reflect muscle coordination at the time scale of the task. Therefore, our results presenting a relationship between patterns of functional muscle coordination (as determined by each distinct task) and shared neural drive (as measured by intermuscular coherence) likely reflect a true underlying prescriptive neural strategy for control.

It is also important to mention that understanding the neural underpinnings of muscle coordination, especially in the context of “muscle synergies” (Brock and Valero-Cuevas 2016; Kutch and Valero-Cuevas 2012; Tresch and Jarc 2009), has been of great interest for many years. The recent application of intermuscular coherence analysis to this field of study is a promising endeavor. However, the entire notion is flawed if the neural binding measured by coherence analysis is found to be unrelated to, or unaffected by, the physical functional coordination among muscles.

It is with this in mind that our study begins to answer important questions concerning the relationship between shared neural drive, as estimated by coherence analysis, and task-driven muscle coordination. We propose that several principles emerge from our results.

The task-dependent strength and timing of EMG amplitude correlations between muscles is predictive of higher frequency intermuscular coherence. Based on previous literature attributing changes in coherence across muscles to the “type of task” (Boonstra et al. 2015; de Vries et al. 2016; Kilner et al. 1999; Kristeva-Feige et al. 2002), it is reasonable to expect that task features such as difficulty, precision requirements, movement, etc. should be of importance. Our results suggest that this list must also include the specific type of muscle coordination required to meet the constraints of a given task. For example, the FDI and APB muscle pair showed the highest coherence during dial rotation, when their synergistic coordination was functionally-relevant for the task of moving the fingertips, and when their EMGs were strongly and positively correlated (Fig. 2). Similarly, the FDS and FDI also showed the highest EMG coherence when they were more functionally synergistic (during the isometric force task) and when their EMGs were also strongly and positively correlated (Fig. 3). Conversely, the EMGs of the FDS and APB muscles were weakly and negatively correlated in both tasks, and their coherence was also weak and varied little across tasks. This evidence shows a strong association between strong/positive EMG amplitude correlations and high intermuscular coherence. This relationship was found regardless of whether muscles were engaged in

isometric force scaling or dial rotation (finger movement) or even if they act anatomically on the same digit or not.

Intermuscular coherence in the beta band does not require steady-state force output and is not abolished by movement. Coherence in the beta band (16–29 Hz) is thought to be very sensitive to movement and dynamic force production. Between the APB and FDI muscles, Kilner et al. (1999) found that ~20 Hz coherence decreased during the movement phase of a dynamic pinching task (Kilner et al. 1999). Even a history of movement has the potential to change beta-band coherence between these muscles (Nazarpour et al. 2012; Omlor et al. 2011). Here, we found no reduction in APB to FDI beta coherence during dial rotation, when a reduction would have been expected as per the literature, since cyclical dial rotation involves both digit movement and dynamic muscle activation. Functionally, beta-band neural drive is thought to play a role in the maintenance of static, isometric force (Aumann and Prut 2015; Kilner et al. 1999; Pogosyan et al. 2009). Production of time-varying muscle force (Omlor et al. 2007; Patino et al. 2008) or isotonic contractions (Gwin and Ferris 2012) shift neural drive away from the beta-band toward higher frequencies (30–50 Hz). As might be expected, our dynamic tasks did not produce distinct peaks in beta-band coherence across muscles. However, beta-band coherence was still present and yet was not highly modulated by task. Our findings of weakly-modulation beta-band intermuscular neural drive suggest that this band lacks functional importance in our dynamic tasks. Even so, others have observed a reduction in beta-band coherence with movement, where we did not (Kilner et al. 1999). The apparent disagreement may simply stem from the different type of muscle coordination required for dial rotation (which obligates synchronous activation of the APB and FDI to simultaneously produce pinch force while ad-abducting the thumb and index finger), as compared with the squeezing together of two levers (as when using a clothespin, where the APB does not contribute to the flexion-adduction movement of the thumb). A neuromechanical interpretation would explain both results. That is, movement reduces beta-band intermuscular drive only when it forces a more individuated control of each muscle. A recent work from our laboratory demonstrates that individuated control of finger muscles is detrimental to beta-band intermuscular coherence, even without overt movement (Reyes et al. 2017).

A ~40 Hz, intermuscular “Piper rhythm” can be evoked consistently by the mechanical requirements of dial rotation. The strong coherence peak at ~40 Hz that was consistently observed between the FDI and APB muscles during dial rotation reflects the so-called Piper rhythm first described in early studies (Brown et al. 1998; von Piper 1907; Tscharner et al. 2011). Although the weaker 30- to 50-Hz coherence observed in other conditions may reflect the same underlying neural drive, it is clear that the FDI APB muscle pair was especially associated with an ~40-Hz coherence and only during dial rotation. The Piper rhythm is particularly relevant because it has been shown to be dopamine dependent (McAuley et al. 2001) and has been suggested as a potential biomarker for Parkinson’s disease. It is therefore also very significant that we have quantified shared neural drive at these frequencies using intermuscular coherence analysis. Previously employed techniques to detect the Piper rhythm focused on individual muscles (e.g., measuring EMG power spectra (McAuley et al. 2001; von

Tscharner et al. 2011), fingertip acceleration (McAuley et al. 2001), or MEG-EMG coherence (Brown et al. 1998). It is more difficult to establish normative baseline values for such measures because of the high intersubject variability in EEG/MEG and EMG signals and the potential for physical differences in limb/muscle size and composition to influence direct measures of EMG or acceleration. Intermuscular coherence, by comparison, should depend less on such factors and has gained popularity as a clinically applicable biomarker in, for example, the evaluation dystonia (Grosse et al. 2004) or primary lateral sclerosis (Fisher et al. 2012). The reason for the consistent emergence of a strong Piper rhythm for just the FDI-APB muscle pair during dial rotation requires further biomechanical exploration, but it may be that the actions of these muscles are critical to the coordination of simultaneous thumb and index finger ad-abduction while also controlling pinch force (Rácz et al. 2012).

Intermuscular coherence in the ~10-Hz range depends on task-dependent coordination among muscles. Traditionally, intramuscular coherence near ~10 Hz is thought to reflect Ia afferent feedback through the stretch reflex loop (Christakos et al. 2006; Erimaki and Christakos 2008; Lippold 1970). Coordination of ~10-Hz input across antagonist muscles of the finger has been shown during slow movements (Vallbo and Wessberg 1993), and coherence at ~10 Hz has been found across many muscles, even between muscles of different hands, where its strength is modulated by the degree of required coupling between muscles (de Vries et al. 2016). Potentially, there is a system within the spinal cord that acts, in a task-dependent way, to connect the afferent feedback generated by each functionally linked muscle. Spinal networks of interneurons are a likely candidate for organizing afferent signals in this way. For example, spinal contributions to coordination among muscles are well characterized in frogs (Hart and Giszter 2010; Kargo and Giszter 2000; Tresch et al. 1999) and mice (Levine et al. 2014). In our tasks, the strongest intermuscular coherence at ~10 Hz was found whenever strong, positive correlations among their EMG signals were present. Given that 10 Hz coupling between muscles is not thought to stem from cortical binding, a reasonable interpretation for our results is that it can serve as an index of subcortical, perhaps even spinal, binding between functionally linked muscles.

Lastly, understanding how functional coordination between muscles influences their shared neural drive (Boonstra et al. 2009; DeMarchis et al. 2015) may be critical for investigating the neural basis of muscle synergies. Specifically, coherence analysis may help to separate synergies which emerge from the mechanical constraints of a task (i.e., “descriptive”) from those that reflect a deliberate neural strategy for muscle coordination (i.e., “prescriptive”) (Brock and Valero-Cuevas 2016). We conclude that our results support the notion that intermuscular coherence is an important tool to evaluate healthy or dysfunctional patterns of coordinated neural drive across muscles.

ACKNOWLEDGMENTS

We thank Dr. Jun Yong Shin for assistance in creating the three-dimensionally printed dial used in this study.

The content is solely the responsibility of the authors and does not necessarily represent the official views of the National Institutes of Health.

GRANTS

Research reported in this publication was supported by the National Institute of Arthritis and Musculoskeletal and Skin Diseases Grants R01-AR-050520 and R01-AR-052345.

DISCLOSURES

No conflicts of interest, financial or otherwise, are declared by the authors.

AUTHOR CONTRIBUTIONS

C.M.L. and F.J.V.-C. conceived and designed research; C.M.L. performed experiments; C.M.L. analyzed data; C.M.L. and F.J.V.-C. interpreted results of experiments; C.M.L. prepared figures; C.M.L. drafted manuscript; C.M.L. and F.J.V.-C. edited and revised manuscript; C.M.L. and F.J.V.-C. approved final version of manuscript.

REFERENCES

- Aumann TD, Prut Y. Do sensorimotor β -oscillations maintain muscle synergy representations in primary motor cortex? *Trends Neurosci* 38: 77–85, 2015. doi:10.1016/j.tins.2014.12.002.
- Baker SN, Pinches EM, Lemon RN. Synchronization in monkey motor cortex during a precision grip task. II. effect of oscillatory activity on corticospinal output. *J Neurophysiol* 89: 1941–1953, 2003. doi:10.1152/jn.00832.2002.
- Bizzi E, Cheung VC. The neural origin of muscle synergies. *Front Comput Neurosci* 7: 51, 2013. doi:10.3389/fncom.2013.00051.
- Bokil H, Purpura K, Schoffelen JM, Thomson D, Mitra P. Comparing spectra and coherences for groups of unequal size. *J Neurosci Methods* 159: 337–345, 2007. doi:10.1016/j.jneumeth.2006.07.011.
- Boonstra TW. The potential of corticomuscular and intermuscular coherence for research on human motor control. *Front Hum Neurosci* 7: 855, 2013. doi:10.3389/fnhum.2013.00855.
- Boonstra TW, Breakspear M. Neural mechanisms of intermuscular coherence: implications for the rectification of surface electromyography. *J Neurophysiol* 107: 796–807, 2012. doi:10.1152/jn.00066.2011.
- Boonstra TW, Daffertshofer A, Roerdink M, Flipse I, Groenewoud K, Beek PJ. Bilateral motor unit synchronization of leg muscles during a simple dynamic balance task. *Eur J Neurosci* 29: 613–622, 2009. doi:10.1111/j.1460-9568.2008.06584.x.
- Boonstra TW, Danna-Dos-Santos A, Xie HB, Roerdink M, Stins JF, Breakspear M. Muscle networks: connectivity analysis of EMG activity during postural control. *Sci Rep* 5: 17830, 2015. doi:10.1038/srep17830.
- Brock O, Valero-Cuevas F. Transferring synergies from neuroscience to robotics: comment on “Hand synergies: Integration of robotics and neuroscience for understanding the control of biological and artificial hands” by M. Santello et al. *Phys Life Rev* 17: 27–32, 2016. doi:10.1016/j.plrev.2016.05.011.
- Brown P, Salenius S, Rothwell JC, Hari R. Cortical correlate of the Piper rhythm in humans. *J Neurophysiol* 80: 2911–2917, 1998.
- Brown SH, Brookham RL, Dickerson CR. High-pass filtering surface EMG in an attempt to better represent the signals detected at the intramuscular level. *Muscle Nerve* 41: 234–239, 2010. doi:10.1002/mus.21470.
- Christakos CN, Papadimitriou NA, Erimaki S. Parallel neuronal mechanisms underlying physiological force tremor in steady muscle contractions of humans. *J Neurophysiol* 95: 53–66, 2006. doi:10.1152/jn.00051.2005.
- Conway BA, Halliday DM, Farmer SF, Shahani U, Maas P, Weir AJ, Rosenberg JR. Synchronization between motor cortex and spinal motoneuronal pool during the performance of a maintained motor task in man. *J Physiol* 489: 917–924, 1995. doi:10.1113/jphysiol.1995.sp021104.
- De Luca CJ, LeFever RS, McCue MP, Xenakis AP. Control scheme governing concurrently active human motor units during voluntary contractions. *J Physiol* 329: 129–142, 1982. doi:10.1113/jphysiol.1982.sp014294.
- De Marchis C, Severini G, Castronovo AM, Schmid M, Conforto S. Intermuscular coherence contributions in synergistic muscles during pedaling. *Exp Brain Res* 233: 1907–1919, 2015. doi:10.1007/s00221-015-4262-4.
- de Vries IE, Daffertshofer A, Stegeman DF, Boonstra TW. Functional connectivity in the neuromuscular system underlying bimanual coordination. *J Neurophysiol* 116: 2576–2585, 2016. doi:10.1152/jn.00460.2016.
- Erimaki S, Christakos CN. Coherent motor unit rhythms in the 6–10 Hz range during time-varying voluntary muscle contractions: neural mechanism and

- relation to rhythmical motor control. *J Neurophysiol* 99: 473–483, 2008. doi:10.1152/jn.00341.2007.
- Farina D, Negro F, Jiang N.** Identification of common synaptic inputs to motor neurons from the rectified electromyogram. *J Physiol* 591: 2403–2418, 2013. doi:10.1113/jphysiol.2012.246082.
- Farina D, Negro F, Muceli S, Enoka RM.** Principles of motor unit physiology evolve with advances in technology. *Physiology (Bethesda)* 31: 83–94, 2016. doi:10.1152/physiol.00040.2015.
- Farmer SF.** Rhythmicity, synchronization and binding in human and primate motor systems. *J Physiol* 509: 3–14, 1998. doi:10.1111/j.1469-7793.1998.003bo.x.
- Farmer SF, Bremner FD, Halliday DM, Rosenberg JR, Stephens JA.** The frequency content of common synaptic inputs to motoneurons studied during voluntary isometric contraction in man. *J Physiol* 470: 127–155, 1993. doi:10.1113/jphysiol.1993.sp019851.
- Fisher KM, Zaaïmi B, Williams TL, Baker SN, Baker MR.** Beta-band intermuscular coherence: a novel biomarker of upper motor neuron dysfunction in motor neuron disease. *Brain* 135: 2849–2864, 2012. doi:10.1093/brain/aws150.
- Giszter SF.** Motor primitives—new data and future questions. *Curr Opin Neurobiol* 33: 156–165, 2015. doi:10.1016/j.conb.2015.04.004.
- Grosse P, Edwards M, Tijssen MA, Schrag A, Lees AJ, Bhatia KP, Brown P.** Patterns of EMG-EMG coherence in limb dystonia. *Mov Disord* 19: 758–769, 2004. doi:10.1002/mds.20075.
- Gwin JT, Ferris DP.** Beta- and gamma-range human lower limb corticomuscular coherence. *Front Hum Neurosci* 6: 258, 2012. doi:10.3389/fnhum.2012.00258.
- Hart CB, Giszter SF.** A neural basis for motor primitives in the spinal cord. *J Neurosci* 30: 1322–1336, 2010. doi:10.1523/JNEUROSCI.5894-08.2010.
- Kakuda N, Nagaoka M, Wessberg J.** Common modulation of motor unit pairs during slow wrist movement in man. *J Physiol* 520: 929–940, 1999. doi:10.1111/j.1469-7793.1999.00929.x.
- Kargo WJ, Giszter SF.** Rapid correction of aimed movements by summation of force-field primitives. *J Neurosci* 20: 409–426, 2000.
- Keenan KG, Santos VJ, Venkadesan M, Valero-Cuevas FJ.** Maximal voluntary fingertip force production is not limited by movement speed in combined motion and force tasks. *J Neurosci* 29: 8784–8789, 2009. doi:10.1523/JNEUROSCI.0853-09.2009.
- Kilner JM, Baker SN, Salenius S, Jousmäki V, Hari R, Lemon RN.** Task-dependent modulation of 15–30 Hz coherence between rectified EMGs from human hand and forearm muscles. *J Physiol* 516: 559–570, 1999. doi:10.1111/j.1469-7793.1999.0559v.x.
- Kristeva-Feige R, Fritsch C, Timmer J, Lücking CH.** Effects of attention and precision of exerted force on beta range EEG-EMG synchronization during a maintained motor contraction task. *Clin Neurophysiol* 113: 124–131, 2002. doi:10.1016/S1388-2457(01)00722-2.
- Kutch JJ, Valero-Cuevas FJ.** Challenges and new approaches to proving the existence of muscle synergies of neural origin. *PLOS Comput Biol* 8: e1002434, 2012. doi:10.1371/journal.pcbi.1002434.
- Lachaux JP, Rodriguez E, Martinerie J, Varela FJ.** Measuring phase synchrony in brain signals. *Hum Brain Mapp* 8: 194–208, 1999. doi:10.1002/(SICI)1097-0193(1999)8:4<194::AID-HBM4>3.0.CO;2-C.
- Laine CM, Martínez-Valdes E, Falla D, Mayer F, Farina D.** Motor neuron pools of synergistic thigh muscles share most of their synaptic input. *J Neurosci* 35: 12207–12216, 2015. doi:10.1523/JNEUROSCI.0240-15.2015.
- Laine CM, Yavuz ŞU, Farina D.** Task-related changes in sensorimotor integration influence the common synaptic input to motor neurons. *Acta Physiol (Oxf)* 211: 229–239, 2014. doi:10.1111/apha.12255.
- Levine AJ, Hinckley CA, Hilde KL, Driscoll SP, Poon TH, Montgomery JM, Pfaff SL.** Identification of a cellular node for motor control pathways. *Nat Neurosci* 17: 586–593, 2014. doi:10.1038/nn.3675.
- Lippold OC.** Oscillation in the stretch reflex arc and the origin of the rhythmical, 8–12 C-S component of physiological tremor. *J Physiol* 206: 359–382, 1970. doi:10.1113/jphysiol.1970.sp009018.
- Mah CD, Mussa-Ivaldi FA.** Evidence for a specific internal representation of motion-force relationships during object manipulation. *Biol Cybern* 88: 60–72, 2003. doi:10.1007/s00422-002-0347-9.
- McAuley JH, Corcos DM, Rothwell JC, Quinn NP, Marsden CD.** Levodopa reversible loss of the Piper frequency oscillation component in Parkinson's disease. *J Neurol Neurosurg Psychiatry* 70: 471–476, 2001. doi:10.1136/jnnp.70.4.471.
- McAuley JH, Marsden CD.** Physiological and pathological tremors and rhythmic central motor control. *Brain* 123: 1545–1567, 2000. doi:10.1093/brain/123.8.1545.
- Mima T, Hallett M.** Corticomuscular coherence: a review. *J Clin Neurophysiol* 16: 501–511, 1999. doi:10.1097/00004691-199911000-00002.
- Nazarpour K, Barnard A, Jackson A.** Flexible cortical control of task-specific muscle synergies. *J Neurosci* 32: 12349–12360, 2012. doi:10.1523/JNEUROSCI.5481-11.2012.
- Omlor W, Patino L, Hepp-Reymond MC, Kristeva R.** Gamma-range corticomuscular coherence during dynamic force output. *Neuroimage* 34: 1191–1198, 2007. doi:10.1016/j.neuroimage.2006.10.018.
- Omlor W, Patino L, Mendez-Balbuena I, Schulte-Mönting J, Kristeva R.** Corticospinal beta-range coherence is highly dependent on the pre-stationary motor state. *J Neurosci* 31: 8037–8045, 2011. doi:10.1523/JNEUROSCI.4153-10.2011.
- Patino L, Omlor W, Chakarov V, Hepp-Reymond MC, Kristeva R.** Absence of gamma-range corticomuscular coherence during dynamic force in a deafferented patient. *J Neurophysiol* 99: 1906–1916, 2008. doi:10.1152/jn.00390.2007.
- Piper HU.** Über den willkürlichen muskeltetanus. *Pflügers Gesamte Physiol Menschen Tiere* 119: 301–338, 1907.
- Pogosyan A, Gaynor LD, Eusebio A, Brown P.** Boosting cortical activity at beta-band frequencies slows movement in humans. *Curr Biol* 19: 1637–1641, 2009. doi:10.1016/j.cub.2009.07.074.
- Potvin JR, Brown SH.** Less is more: high pass filtering, to remove up to 99% of the surface EMG signal power, improves EMG-based biceps brachii muscle force estimates. *J Electromyogr Kinesiol* 14: 389–399, 2004. doi:10.1016/j.jelekin.2003.10.005.
- Rácz K, Brown D, Valero-Cuevas FJ.** An involuntary stereotypical grasp tendency pervades voluntary dynamic multifinger manipulation. *J Neurophysiol* 108: 2896–2911, 2012. doi:10.1152/jn.00297.2012.
- Reyes A, Laine CM, Kutch JJ, Valero-Cuevas FJ.** Beta band corticomuscular drive reflects muscle coordination strategies. *Front Comput Neurosci* 11: 17, 2017. doi:10.3389/fncom.2017.00017.
- Riley ZA, Terry ME, Mendez-Villanueva A, Litsey JC, Enoka RM.** Motor unit recruitment and bursts of activity in the surface electromyogram during a sustained contraction. *Muscle Nerve* 37: 745–753, 2008. doi:10.1002/mus.20978.
- Rosenberg JR, Amjad AM, Breeze P, Brillinger DR, Halliday DM.** The Fourier approach to the identification of functional coupling between neuronal spike trains. *Prog Biophys Mol Biol* 53: 1–31, 1989. doi:10.1016/0079-6107(89)90004-7.
- Sears TA, Stagg D.** Short-term synchronization of intercostal motoneurone activity. *J Physiol* 263: 357–381, 1976. doi:10.1113/jphysiol.1976.sp011635.
- Semmler JG, Kornatz KW, Dinno DV, Zhou S, Enoka RM.** Motor unit synchronisation is enhanced during slow lengthening contractions of a hand muscle. *J Physiol* 545: 681–695, 2002. doi:10.1113/jphysiol.2002.026948.
- Staudenmann D, Potvin JR, Kingma I, Stegeman DF, van Dieën JH.** Effects of EMG processing on biomechanical models of muscle joint systems: sensitivity of trunk muscle moments, spinal forces, and stability. *J Biomech* 40: 900–909, 2007. doi:10.1016/j.jbiomech.2006.03.021.
- Tresch MC, Jarc A.** The case for and against muscle synergies. *Curr Opin Neurobiol* 19: 601–607, 2009. doi:10.1016/j.conb.2009.09.002.
- Tresch MC, Saltiel P, Bizzi E.** The construction of movement by the spinal cord. *Nat Neurosci* 2: 162–167, 1999. doi:10.1038/5721.
- Valero-Cuevas FJ.** Predictive modulation of muscle coordination pattern magnitude scales fingertip force magnitude over the voluntary range. *J Neurophysiol* 83: 1469–1479, 2000.
- Valero-Cuevas FJ, Zajac FE, Burgar CG.** Large index-fingertip forces are produced by subject-independent patterns of muscle excitation. *J Biomech* 31: 693–703, 1998. doi:10.1016/S0021-9290(98)00082-7.
- Vallbo AB, Wessberg J.** Organization of motor output in slow finger movements in man. *J Physiol* 469: 673–691, 1993. doi:10.1113/jphysiol.1993.sp019837.
- Venkadesan M, Valero-Cuevas FJ.** Neural control of motion-to-force transitions with the fingertip. *J Neurosci* 28: 1366–1373, 2008. doi:10.1523/JNEUROSCI.4993-07.2008.
- von Tscharnar V, Barandun M, Stirling LM.** Piper rhythm of the electromyograms of the abductor pollicis brevis muscle during isometric contractions. *J Electromyogr Kinesiol* 21: 184–189, 2011. doi:10.1016/j.jelekin.2010.10.004.
- Ward NJ, Farmer SF, Berthouze L, Halliday DM.** Rectification of EMG in low force contractions improves detection of motor unit coherence in the beta-frequency band. *J Neurophysiol* 110: 1744–1750, 2013. doi:10.1152/jn.00296.2013.
- Zajac FE.** Muscle and tendon: properties, models, scaling, and application to biomechanics and motor control. *Crit Rev Biomed Eng* 17: 359–411, 1989.